Photonic Generation of Ultrawideband (UWB) Pulse With Tunable Notch-Band Behavior

Jianyu Zheng, Ninghua Zhu, Lixian Wang, Jianguo Liu, and Honggang Liang

State Key Laboratory on Integrated Optoelectronics, Institute of Semiconductors, Chinese Academy of Sciences, Beijing 100083, China

DOI: 10.1109/JPHOT.2012.2193562
1943-0655/$31.00 ©2012 IEEE

Manuscript received February 28, 2012; revised March 27, 2012; accepted March 29, 2012. Date of current version April 20, 2012. This work was supported in part by the Major Program of the National Natural Science Foundation of China under Grant 61090390, by the National Basic Research Program of China under Grant 2012CB315702, by the Foundation for Innovative Research Groups of the National Natural Science Foundation of China under Grant 61021003, by the Funds for International Cooperation and Exchange of the National Natural Science Foundation of China under Grant 60820106004, and by the Chinese Academy of Sciences (CAS) Special Grant for Postgraduate Research, Innovation, and Practice. Corresponding author: J. Liu (e-mail: jgliu@semi.ac.cn).

Abstract: A photonic approach to generating the ultrawideband (UWB) pulses with tunable band-rejection behavior based on a negative coefficient two-tap microwave photonic filter is proposed and experimentally demonstrated. To avoid the interference between UWB and the Wireless Fidelity system, the UWB pulse with the "batwing" shape, which corresponds to the 5-GHz notch-band in frequency domain, is generated. Moreover, the band-notched position of the generated UWB signals could be tuned by adjusting the basic delay of the microwave photonic filter. Utilizing the optically tunable band-rejection character, the UWB systems can coexist with existing and future wireless network technologies almost without interference, as well as provide the opportunity for the combination between UWB-over-fiber and cognitive radio.

Index Terms: Ultrawideband radio, microwave photonic filtering, cognitive radio-over-fiber.

1. Introduction

Ultrawideband (UWB) technology is at present defined by the Federal Communications Commission (FCC) as any wireless transmission scheme that occupies a fractional bandwidth $\Delta f/f_0 \geq 20\%$, where Δf is the -10-dB bandwidth, and f_0 is the center frequency of signal, or more than 500 MHz of absolute bandwidth [1]. Due to immunity to multipath fading, low power consumption, and high range resolution, UWB technology is considered promising for high-speed indoor wireless communication systems and sensor networks [2], [3].

Most research about UWB technology over the past few years has been focused on two issues. The first one is how to extend the short coverage range which is result from the ultralow average transmit power of the UWB signals. A feasible solution to this issue is UWB-over-fiber [4], where it is promising for the UWB signals being generated in optical domain at the center office and then distributed to remote base-stations by a long haul optical fiber. In 2006, Yao *et al.* demonstrated a method to generate an UWB doublet utilizing electrooptic intensity modulator that is biased at the nonlinear regime [5]. The methods utilizing the phase-modulation to intensity-modulation (PM–IM) conversion, which is realized by employing the optical phase modulator or high-nonlinear fiber and the photonic discriminator, such as fiber Bragg gating and silicon microring, to finally generate UWB

one or two order Gaussian pulse, were reported between 2006 to 2010 [6]–[9]. Bolea *et al.* demonstrated a UWB pulse generator based on an N-tap microwave photonic filter fed by a laser array [10]. Lee *et al.* proposed and experimentally demonstrated an alternative photonic scheme for the generation of UWB doublet pulses, which is based on an optical fiber-based nonlinear optical loop mirror incorporating the optical parametric amplification effect [11]. The Chaotic-UWB signals generated based on the nonlinear dynamics of laser diode with optical feedback and injection was demonstrated in [12] and [13].

Another issue about UWB technology is how to avoid interference between the UWB signals and other existing narrowband (NB) radio frequency signals resulting from spectrum overlay between them [14]. For example, the operational frequency of the Wireless Fidelity (Wi-Fi) system is 5 GHz, which is located at the spectrum range of the UWB signals. To avoid the interference between UWB and Wi-Fi systems, a series of UWB antennas and filters with specific notch-band around 5 GHz were designed and fabricated [15]–[19], but the fixed notch-band of these components limits them be used in the complicate environment. Actually, a perfect approach to solve the interference problem is the Cognitive UWB Radio [20], which could not only avoid the interference due to the spectrum overlay between UWB and NB communication systems but improve the spectrum efficiency remarkably as well. Nevertheless, the dynamic control for the spectra of the UWB signals, which is the key for implementing the dynamic spectrum access in the cognitive radio (CR), is still a challenge because of the limited processing speed of the analog-to-digital (A/D) and digital-to-analog (D/A) converters [20].

In this paper, we propose and experimentally demonstrate a method of optically generating the UWB signals with a tunable notch-band for the first time. In our experiment, a negative coefficient two-tap microwave photonic filter, which is mainly composed of a phase modulator (PM), a dense wave division multiplexing (DWDM) add-drop thin film filer, and two photodetectors (PDs), was applied in order to filter the particular frequency components of the generated UWB signals. The UWB pulse with the "batwing" shape, which corresponds to the 5-GHz notch-band in frequency domain, was generated. Moreover, the band-notched position of the UWB signals could be tuned from 3.125 GHz to 8.125 GHz through adjusting the basic delay of the microwave photonic filter. The UWB signals with tunable band-rejection characteristic generated in our experiment could avoid the application of the specially designed filters or antennas at the base-stations, as well as provide the opportunity for the combination between UWB-over-fiber and CR.

2. Experimental Setup and Operation Principle

Fig. 1 shows the experimental setup of the proposed approach. A continuous-wave tunable laser diode (TLD) is employed to emit the light. The light is injected to the PM with a 3-dB bandwidth of 40 GHz after through the polarization controller (PC). An electrical pulse train is generated from a pulse pattern generator (PPG) which cascades a 7.8-GHz electrical low-pass filter (LPF) to smooth the initial electrical pulse for obtaining a Gaussian-like profile. The Gaussian-like electrical pulses are amplified by an electrical amplifier (max gain $g = 26$ dB, frequency span from 40 kHz to 38 GHz), and then drive the PM with a fixed pattern "0000 0000 0000 0001" (one "1" per 16 bits) at a bit rate of 10 Gb/s, indicating that the pulse repetition rate is 625 MHz and the full-width at half-maximum (FWHM) is about 85 ps. Therefore, the temporal phase of the output light from PM varies along with the drove Gaussian electrical pulse, thus lead to a chirp with a monocycle profile which is just described by the first-order derivative of Gaussian function. A DWDM add-drop thin film filter with 100-GHz channel separations is inserted after the PM, in which the different wavelength components of the modulated light will be selected into the reflected and passed ports, respectively, when the center wavelength of the light emitted from TLD is set at a suitable value. As shown in the left inset of Fig. 1, there are two cross-points "A" and "B" between the transfer response curves of the passed port (solid line) and reflected port (dash line). If the operating frequency (or wavelength) of the modulated light is aligned with the linear region around point "A" or "B," the optical UWB monocycle pulses with the reversed polarities will be converted from the chirp with the monocycle profile at the two ports of the DWDM filter (see the inset of Fig. 1), which will be converted to

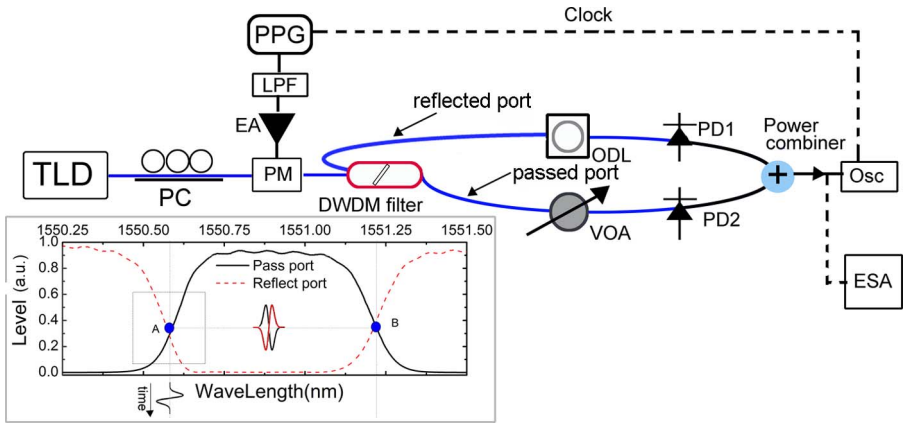

Fig. 1. Experimental setup for photonic UWB pulse generation with tunable notch-band behavior. TLD: Tunable laser diode. PC: Polarization controller. PM: Phase modulator. PPG: Pulse pattern generator. LPF: Low pass filter. EA: Electrical amplifier. DWDM filter: dense wavelength-division-multiplexing add-drop thin film filter. ODL: Optical delay line. OVA: Optical variable attenuator. PD: Photodetector. Osc: Oscilloscope. ESA: electrical spectrum analyzer. Inset: transmission function of DWDM filter and schematic diagram of the PM-to-IM conversion.

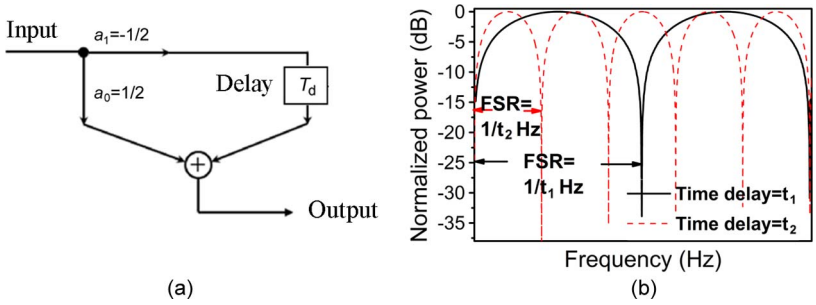

Fig. 2. (a) Equivalent model of negative coefficient two-tap notch filter and (b) transfer response curves at different time delay.

electrical UWB signals by the PD1 and PD2. Finally, the electrical UWB pulse with a particular profile will be synthesized from the two UWB monocycle pulses by the power combiner. In order to control the relative delay time and balance the intensity between the optical signals output from two ports, the optical delay line (ODL) and variable optical attenuator (VOA) are put before the PDs, respectively. A 50-GHz sampling oscilloscope (Osc) and a 40-GHz electrical spectrum analyzer (ESA) are used to measure and record the waveforms and power spectra of the generated UWB signals.

As mentioned above, while the varied frequency (or wavelength) of the chirp is aligned with the linear regions of the response functions of the DWDM filter by adjusting the TLD's operating wavelength, a negative coefficient two-tap microwave photonic filter is formed in the experiment setup, whose equivalent model is presented in Fig. 2(a), and a transfer function is given by [21]

$$H(f) = a_0 + a_1 \cdot \exp(-j2\pi f T_d) \tag{1}$$

where f is the frequency of the signals, and a_0 and a_1 are the filter taps coefficients with opposite sign. The basic delay of the filter T_d corresponds to the relative delay time between the signals output from passed and reflected ports which could be changed by adjusting the ODL in our

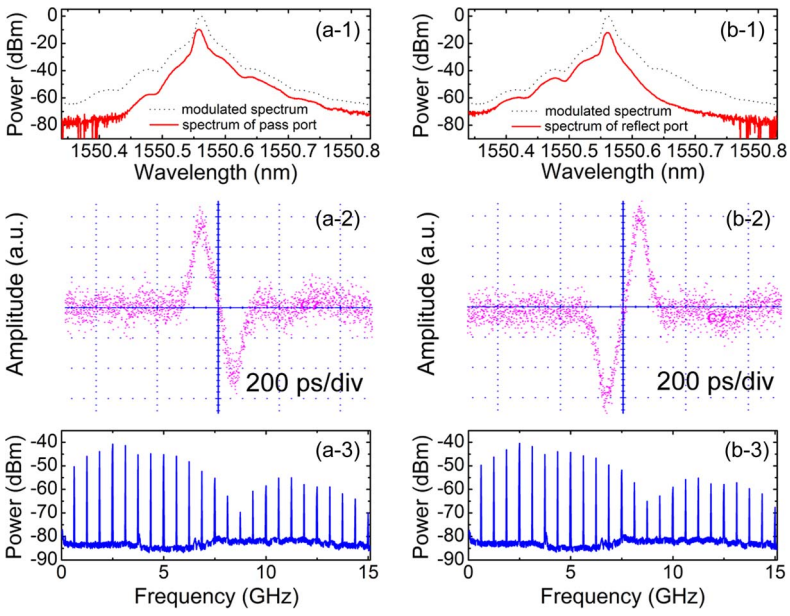

Fig. 3. Optical spectra, waveforms, and rf spectra of the polarity-reversed monocycle pulses output from (a) passed port and (b) reflected port of the DWDM filter.

experiment. As the operating wavelength of TLD is fixed at point "A" or "B" and the insert loss of the DWDM filter and ODL is neglected, the frequency response of the filter can be expressed as

$$H(f) = 1/2(1 - \exp(-j2\pi f T_d)) \tag{2}$$

which was plotted in Fig. 2(b) as $T_d = t_1$ (solid line) and $T_d = t_2$ (dash line). As we have seen, the notched band occurs periodically at different frequency positions, which could be varied by tuning the ODL due to the free spectral range (FSR) corresponds to the invert of basic delay. Hence, the UWB signal with tunable notch-band characteristics is expected to be generated based on our method.

3. Experiment Results

The optical spectra, waveforms and rf spectra of the UWB monocycle pulses generated at output ports of the DWDM filter was investigated as the operating wave of the TLD is fixed at 1550.560 nm (point "A"), which are summarized at Fig. 3. Fig. 3(a) and (b) display the results output from passed port and reflected port, respectively. As shown in Fig. 3(a-1) and (b-1), the lower and upper sidebands of the optical spectrum of the modulated light was filtered out at the two ports symmetrically, which means that the PM-to-IM conversion was implemented successfully. The pulse duration of the polarity-reversed monocycle pulses is about 100 ps whose waveforms own symmetrical profile [see Fig. 3(a-2) and (b-2)]. Due to the periodicity of the original electrical pulse train from PPG, the measured rf spectra are all discrete with a frequency spacing of 625 MHz. Fig. 3(a-3) and (b-3) show that the −10-dB bandwidths of the two types of UWB pulses both are up to 6.50 GHz. The approximate rf spectrum shape of the UWB signals also indicates that the other parameters of the generated monocycle pulses are same, except for their polarities.

The UWB signals with band-notched behavior could be synthesized by the power combiner because of the notch effect of the microwave photonic filter. The UWB signals with notched band at 5 GHz were obtained as the relative delay time was set at 200 ps, whose rf spectrum and waveform are described in Fig. 4. As can be seen from Fig. 4(a), the rf spectrum of the obtained UWB signals

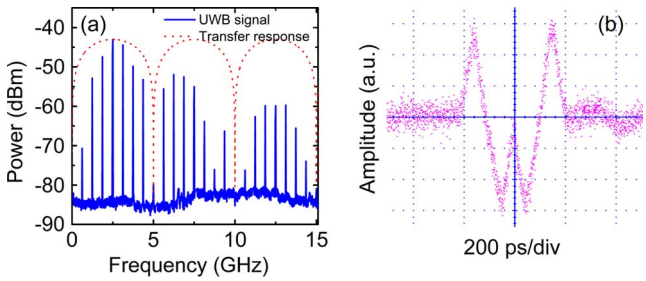

Fig. 4. (a) Rf spectrum of the UWB signals with 5-GHz band-rejection and (b) corresponding waveform.

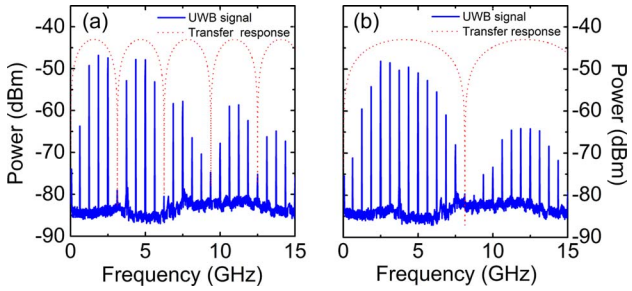

Fig. 5. Response curves of the notch filter and rf spectra of the UWB signals as the relative delay time was set at (a) 320 ps or (b) 123 ps.

possess three notches at different frequency position in addition to the 5-GHz notch. The frequency spacing of adjacent notches corresponds to the FSR of the response curve (dot line) of the notched filter. Moreover, the relative rejection depth (RRD) has reached about 35 dB at the frequency position of 5 GHz. The corresponding waveform of the UWB pulse resembles a batwing in profile, as shown in Fig. 4(b), whose pulse duration is about 400 ps. Note that the polarity-reversed UWB signals with the "batwing" shape could be generated when the operating wavelength of the TLD is tuned from point "A" to point "B" displayed in the inset of Fig. 1. Predictably, the spectrum-overlay-induced interference between UWB and Wi-Fi communication systems could be averted completely once the UWB signals displayed in Fig. 4 are applied in practice.

In our experiment, the adjustment of the band-notched position from 3.125 GHz to 8.125 GHz was achieved through adjusting the delay time of the ODL. Fig. 5(a) shows that the UWB signals with multi-band-notches was generated as the relative delay time was set at 320 ps, and the first band-notch occurred at 3.125 GHz. The rf spectrum of UWB pulse with 8.125-GHz band-notch is displayed in Fig. 5(b), which corresponds to the relative delay time of about 123 ps. In fact, the waveform of the UWB pulse with the band-notch of 8.125 GHz is a doublet pulse with the pulse duration of about 323 ps.

The ODL shows an increasing insert loss following the increase of the provided delay time, which will lead to the imbalance of signal intensity between the two arms of the microwave photonic filter and consequently to the deterioration of the notched degree. Rebalancing the optical power of the two ports, i.e., controlling the relative decrement by the VOA, is an available method to optimize the RRD. Fig. 6 describes the RRD at 5 GHz varied as a function of the relative decrement as the T_d was set at 200 ps. The theoretical results are calculated according to (1). It can be seen that the RRD reaches the maximum value as the optical power difference between two arms returns to the balance point (namely the relative decrement equals to 0 dB) and that the experimental results are very well consistent with the theoretical results.

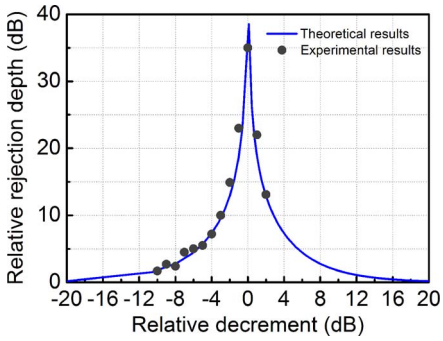

Fig. 6. Relative rejection depth at 5 GHz varied as a function of the relative decrement as $T_d = 200$ ps.

4. Discussion and Conclusion

In the course of TLD's wavelength tuning, the varied frequency of the chirp is likely to drop into the nonlinear region of the DWDM filter's reflected or passed slope as shown in the inset of Fig. 1, which will induce the slight variation of response function of the build-in microwave photonic filter. During the experiment, therefore, we have taken note that the value of RRD was fluctuating in $\pm$2-dB range when the operated wavelength of the TLD was varied from 1550.50 nm to 1550.70 nm artificially. However, the drift of the DWDM filter operating point from the laser wavelength hardly impacts the pulse profile and notch effect of the generated UWB signals because its fluctuated range is very small.

In the proposed setup, the on-off-keying, pulse-amplitude-modulation, pulse-position-modulation, and pulse-polarity-modulation for the band-notched UWB signals could be implemented by coding the Gaussian-like electrical pulse train, because the filtering and coding processes are relatively independent. Moreover, if an intensity modulator substitutes for the VOA in the experiment, the pulse-shape-modulation could be implemented. In addition, two PDs were applied in our experiment in order to avoid the problems associated with optical coherence, which will increase the complexity and cost of the base-stations. However, if another PC is inserted into the passed or reflected port to maintain orthogonality between both optical components output from the ports, the optical UWB signals with reversed polarity could be synthesized in optical domain directly through an optical coupler or optical polarization combiner and converted to electrical signals by a PD in the remote base-station.

In conclusion, an optically band-notched UWB radio generator was proposed and experimentally demonstrated utilizing a negative coefficient two-tap microwave photonic filter which mainly consists of a PM, a DWDM filer, and two PDs. In our experiment, the band-notched position of the UWB signals could be tuned from 3.125 GHz to 8.125 GHz by adjusting the basic delay of the microwave photonic filter. Particularly, the UWB pulse with the "batwing" shape, which corresponds to the 5-GHz band-rejection in frequency domain, was generated in order to avoid the interference between UWB and Wi-Fi system in practice. Such findings are of great potential for applications in cognitive-UWB-over-fiber system, because flexible spectrum-shape conversion makes it convenient to realize dynamic spectrum accessing.

Acknowledgment

The authors would like to acknowledge Dr. J. Man for his inspiring discussions.

References

[1] D. Porcine, P. Research, and W. Hirt, "Ultra-wideband radio technology: Potential and challenges ahead," *IEEE Commun. Mag.*, vol. 41, no. 7, pp. 66–74, Jul. 2003.

[2] S. Roy, J. R. Foerster, V. S. Somayazulu, and D. G. Leeper, "Ultrawideband radio design: The promise of high-speed, short-range wireless connectivity," *Proc. IEEE*, vol. 92, no. 2, pp. 295–311, Feb. 2004.

[3] I. F. Akyildiz, W. Su, Y. Sankarasubramaniam, and E. Cayirci, "A survey on sensor networks," *IEEE Commun. Mag.*, vol. 40, no. 8, pp. 102–114, Aug. 2002.
[4] M. Ran, B. I. Lembrikov, and Y. B. Ezra, "Ultra-wideband radio-over-optical fiber concepts, technologies and applications," *IEEE Photon. J.*, vol. 2, no. 1, pp. 36–48, Feb. 2010.
[5] Q. Wang and J. Yao, "UWB doublet generation using nonlinearly-biased electro-optic intensity modulator," *Electron. Lett.*, vol. 42, no. 22, pp. 1304–1305, Oct. 2006.
[6] F. Zeng and J. Yao, "Ultrawideband impulse radio signal generation using a high-speed electrooptic phase modulator and a fiber-brag-grating-based frequency discriminator," *IEEE Photon. Technol. Lett.*, vol. 18, no. 19, pp. 2062–2065, Oct. 2006.
[7] P. Velanas, A. Bogris, A. Argyris, and D. Syvridis, "High-speed all-optical first- and second-order differentiators based on cross phase modulation in fibers," *J. Lightw. Technol.*, vol. 26, no. 18, pp. 3269–3276, Sep. 2008.
[8] F. Liu, T. Wang, Z. Zhang, M. Qiu, and Y. Su, "On-chip photonic generation of ultra-wideband monocycle pulses," *Electron. Lett.*, vol. 45, no. 24, pp. 1247–1249, Nov. 2009.
[9] X. Feng, Z. Li, B.-O. Guan, C. Lu, H. Y. Tam, and P. K. A. Wai, "Switchable UWB pulse generation using a polarization maintaining fiber Bragg grating as frequency discriminator," *Opt. Exp.*, vol. 18, no. 4, pp. 3643–3648, Feb. 2010.
[10] M. Bolea, J. Mora, B. Ortega, and J. Capmany, "Optical UWB pulse generator using an N tap microwave photonic filter and phase inversion adaptable to different pulse modulation formats," *Opt. Exp.*, vol. 17, no. 7, pp. 5023–5032, Mar. 2009.
[11] J. Lee, Y. M. Chang, and J. H. Lee, "All-optical pulse shaping for ultrawideband doublet pulses using nonlinear optical loop mirror with optical parametric amplification," *Opt. Lett.*, vol. 36, no. 21, pp. 4277–4230, Nov. 2011.
[12] J.-Y. Zheng, M.-J. Zhang, A.-B. Wang, and Y.-C. Wang, "Photonic generation of ultrawideband pulse using semiconductor laser with optical feedback," *Opt. Lett.*, vol. 35, no. 11, pp. 1734–1736, Jun. 2010.
[13] M.-J. Zhang, T.-G. Liu, A.-B. Wang, J.-Y. Zheng, L.-N. Meng, Z.-X. Zhang, and Y.-C. Wang, "Photonic ultrawideband signal generator using an optically injected chaotic semiconductor laser," *Opt. Lett.*, vol. 36, no. 6, pp. 1008–1010, Mar. 2011.
[14] M. Hämäläinen, V. Hovinen, R. Tesi, J. H. J. Iinatti, and M. Latva-aho, "On the UWB system coexistence with GSM900, UMTS/WCDMA, and GPS," *IEEE J. Sel. Areas Commun.*, vol. 20, no. 9, pp. 1712–1721, Dec. 2002.
[15] Y. J. Cho, K. H. Kim, D. H. Choi, S. S. Lee, and S.-O. Park, "A miniature UWB planar monopole antenna with 5-GHz band-rejection filter and the time-domain characteristics," *IEEE Trans. Antennas Propag.*, vol. 54, no. 5, pp. 1453–1460, May 2006.
[16] J. Kim, C. S. Cho, and J. W. Lee, "5.2 GHz notched ultra-wideband antenna using slot-type SRR," *Electron. Lett.*, vol. 42, no. 6, pp. 315–316, Mar. 2006.
[17] K. Bahadori and Y. Rahmat-Samii, "A miniaturized elliptic-card UWB antenna with WLAN band rejection for wireless communications," *IEEE Trans. Antennas Propag.*, vol. 55, no. 11, pp. 3326–3332, Nov. 2007.
[18] P. Mondal and Y. L. Guan, "A coplanar stripline ultra-wideband bandpass filter with notch band," *IEEE Microw. Wireless Compon. Lett.*, vol. 20, no. 1, pp. 22–24, Jan. 2010.
[19] X. Lou, J.-G. Ma, K. Ma, and K. S. Yeo, "Compact UWB bandpass filter with ultra narrow notched band," *IEEE Microw. Wireless Compon. Lett.*, vol. 20, no. 3, pp. 145–147, Mar. 2010.
[20] H. Zhang, X. Zhou, K. Y. Yazdandoost, and I. Chlamtac, "Multiple signal waveforms adaptation in cognitive ultra-wideband radio evolution," *IEEE J. Sel. Areas Commun*, vol. 24, no. 4, pp. 878–884, Apr. 2006.
[21] W. Li, N. H. Zhu, and L. X. Wang, "Continuously tunable microwave photonic notch filter with a complex coefficient," *IEEE Photon. J.*, vol. 3, no. 3, pp. 462–467, Jun. 2011.